BINDING BETWEEN INSULIN-LIKE GROWTH FACTOR 1 AND INSULIN-LIKE GROWTH FACTOR BINDING PROTEIN 3 IS NOT INFLUENCED BY GLUCOSE OR 2-DEOXY-D-GLUCOSE*

Matei Mireuta[1], Mark A. Hancock[2], and Michael Pollak[1]

[1]Segal Cancer Centre, Montreal, QC, Canada, H3T 1E2; [2]Sheldon Biotechnology Centre, McGill University, Montreal, QC, Canada, H3A 2B4

Running head: Effect of glucose and 2-DG on IGF-1/IGFBP-3

Address correspondence to: Michael Pollak, MD, 3755 Cote-Ste Catherine, Montreal, QC, H3T 1E2.

Telephone: 514-340-8222 ext. 4139; Fax: 514-340-8222; Email: michael.pollak@mcgill.ca

A recent report details that 2-deoxy-D-glucose (2-DG), a well known inhibitor of glycolysis and a candidate antineoplastic agent, also induces insulin-like growth factor 1 receptor (IGF-1R) signaling through the inhibition of insulin-like growth factor 1/ insulin-like growth factor binding protein 3 (IGF-1/IGFBP-3) complex formation. The authors hypothesized that disrupted IGF-1/IGFBP-3 binding by 2-DG led to increased free IGF-1 concentrations and, consequently, activation of IGF-1R downstream pathways. Since their report suggests unprecedented off-target effects of 2-DG, this has profound implications for the fields of metabolism and oncology. Using ELISA, surface plasmon resonance (SPR), and novel "intensity-fading" mass spectrometry (MS), we now provide a detailed characterization of complex formation between IGF-1 and IGFBP-3. All three of these independent methods demonstrated that there was no effect of glucose or 2-DG on the interaction between IGF-1 and IGFBP-3. Furthermore, we show examples of 2-DG exposure associated with reduced rather than increased IGF-1R and AKT activation, providing further evidence against a 2-DG increase in IGF-1R activation by IGF-1/IGFBP-3 complex disruption.

Insulin-like Growth Factors I and II (IGF-1, IGF-2) are peptide hormones similar in molecular structure to insulin and they regulate a variety of cellular activities including metabolism, proliferation and growth. Both IGFs bind to the IGF-1 receptor (IGF-1R) at the cell membrane and initiate a signaling cascade that results in the activation of the PI3K/AKT/mTOR (Phosphadityl Inositol 3 Kinase/AKT/ mammalian Target Of Rapamycin) pathway (1-5)(1-5). The IGF-2 receptor (IGF-2 R), which binds to IGF-2, lacks an intracellular signaling domain and is therefore considered to only act as a sink for excess IGF-2 (6).

IGF actions are tightly modulated by a family of proteins called Insulin-like Growth Factor Binding Proteins (IGFBPs), of which IGFBP-1 through 6 have been characterized. Most IGFBPs in the blood originate from the liver, but they are also expressed in many other tissues. IGFBP-3 and 5 are the most abundant IGFBPs in the circulation. They form a ternary complex with IGFs and a third protein termed Acid-Labile Subunit (ALS) (7-9). IGFBPs are known to modulate actions of IGFs both *in vitro* and *in vivo* (7). Since only free IGFs are considered ligands for the IGF-1R, significant research efforts have focused on small molecules capable of interfering with IGF-IGFBP binding.

A recent report showed that 2-deoxy-D-glucose (2-DG), a close derivative of glucose, promoted dissociation of IGF-1 from IGFBP-3 and consequently contributed to elevated phoshoserine 473 AKT levels in a variety of cancer cell lines (10). 2-DG has been proposed as a potential therapeutic agent in the treatment of cancer since it interferes with glycolysis (11). Entering the cell through glucose transporters, 2-DG inhibits enzymes of the glycolytic pathway both competitively (phosphoglucose isomerase) (12) and non-competitively (hexokinase) (13). Since tumor cells depend more heavily on glycolysis compared to normal cells, 2-DG is under investigation for cancer treatment (14).

The recent study by Zhong and co-workers (10) showed that 2-DG, apart from its classic activities as an inhibitor of glycolysis, can also increase IGF-1R signaling by disrupting IGF-1/IGFBP-3 binding. As increased IGF-1R

signaling is associated with greater proliferation of tumor cells, this report has shed doubt on the efficacy of 2-DG as a cancer therapeutic. To examine this issue further, the present study characterizes the effect of glucose and 2-DG on binding between IGF-1 and IGFBP-3. Using ELISA, Surface Plasmon Resonance (SPR), and novel "intensity-fading" Mass Spectrometry (MS), we report that that glucose and 2-DG have no effect on IGF-1/IGFBP-3 complex formation.

Experimental Procedures

Materials – Human recombinant IGF-1 was purchased from Feldan Biosciences (Montreal, Canada) and human recombinant IGFBP-3 was obtained from Insmed Incorporated (Glen Allen, Virginia, USA). Glucose, 2-DG, and fatty-acid free bovine serum albumin (BSA) were purchased from Sigma (Mississauga, Ontario, Canada). MCF-7, T47D and HeLa cell lines were obtained from American Type Culture Collection (ATCC) (Manassas, VA, USA) and cultured in standard DMEM medium supplemented with 10% fetal bovine serum (FBS) and 20 μg/ml Gentamycin.

ELISA – Microtitre plates (Costar, Lowell, MA, USA) were coated with either human recombinant IGF-1 (5μg/ml) or human recombinant IGFBP-3 (2μg/ml) in PBS overnight at room temperature. Plates were washed three times with sample buffer (PBS or HBS-EP; 100μl/well) and then blocked for 3 hours at room temperature using 5% (w/v) casein (in sample buffer; 300μl/well). Plates were washed again in the similar manner before 30 min incubations with IGFBP-3 or 2.5 hour incubations with IGF-1 at room temperature. After washing, primary antibodies (anti-IGFBP-3 or anti IGF-1; Santa Cruz, Santa Cruz, California,USA) were added to each well (100μl of 1:50 dilution in sample buffer containing 5% (w/v) casein) for 1 hour at room temperature. After washing, secondary antibody (Santa Cruz, Santa Cruz, California,USA) was added to each well in the similar manner. After washing, the color developing solution (RnD Systems, Mineapolis, MN, USA) was added to the wells and absorbance readings were monitored at 450 nm.

SPR - Label-free, real-time binding between IGF-1 (7.6 kDa) and IGFBP-3 (29 kDa) was examined using a Biacore 3000 system (GE Healthcare Bio-Sciences, AB, USA) at 25°C with filtered (0.2 μm) and degassed HBS-EP running buffer (10mM HEPES pH 7.4, 150mM NaCl, 3mM EDTA, 0.005% (v/v) Tween20). IGFBP-3 (9 μg/mL in 10 mM sodium acetate pH 5.5) was immobilized to CM4 sensor chips using the Biacore Amine Coupling Kit (~1000 RU final); corresponding reference surfaces were prepared in the absence of IGFBP-3. IGF-1 (0 – 25 nM; or BSA as negative control) was injected over reference and IGFBP-3-immobilized surfaces, in the absence or presence of competitor (25 – 100 mM glucose or 2-DG), using variable flow rates (10-75 μl/min) and contact times (3-5 min association, 5-10 min dissociation). Between sample injections, sensor chip surfaces were regenerated using Pierce Gentle Elution buffer (Thermo Scientific, Illinois, USA) containing 0.1% (v/v) Empigen (Affymetrix-Anatrace, Ohio, USA).

All SPR data was double-referenced (15) and is representative of duplicate injections acquired from two independent trials. For each titration series, a buffer blank (+/- glucose or 2-DG) was injected first, the highest IGF-1 concentration second, and serial dilutions then followed (from the lowest to the highest concentration repeated). Comparing binding responses between the highest IGF-1 injections verified consistent IGFBP-3-immobilized surface activity throughout each assay. Apparent equilibrium dissociation constants (K_D), as well as individual association (k_a) and disscoation (k_d) rate constants, were determined by global fitting of the data to a "1:1 kinetic" model with or without mass transport (BIAevaluation v4.1 software). The kinetic estimates represent fits to the experimental data where Chi^2 values were <1.5.

MS – Eppendorf tubes containing IGF-1 (13μM) or IGF-1 plus IGFBP-3 (13 or 26μM) samples were incubated for 3 hours on a rocking platform at room temperature. A normal phase (NP-20) protein chip (Bio-Rad, Mississauga, ON, Canada) was washed three times with 5 μl of HPLC-grade water before the addition of 5 μl of sample per spot and air drying. Subsequently, each

spot was washed three times with 5µl of a low stringency buffer (Bio-Rad) and then left to air dry. 5 mg of α-Cyano-4-hydroxycinnamic acid (CHCA; Bio-Rad) was dissolved in 200 µl of solution A (50% (v/v) HPLC-grade water, 49.5% (v/v) acetonitrile, and 0.5% (v/v) trifluoroacetic acid); the mixture was vortexed for 5 minutes and then centrifuged for 10 minutes before the supernatant was collected and further diluted with 200 µl of solution A. The diluted supernatant was then added to each spot (1µl per spot) and left to air dry; this was repeated twice to create two layers. The chip was then analyzed using a Ciphergen Protein Chip Series 4000 instrument (Ciphergen Biosystems, Fremont, CA, USA).

Western Blots – Total cell lysates were obtained using RIPA buffer as described earlier (16). 50 µg of total protein were loaded per lane and membranes were immunoblotted with phosphor-serine 473 AKT, AKT, phospho-tyrosine 1135/1136 IGF-1R beta chain, IGF-1R beta chain and β-actin (Cell Signaling, Danvers, MA, USA).

Results

Qualitative binding of IGF-1 to IGFBP-3 – Initially, ELISA assays were performed in which IGF-1 was immobilized in the microtitre wells (Figure 1). In PBS- (data not shown) or HBS-based buffer systems, saturable, dose-dependent binding of IGFBP-3 was detected and yielded sigmoidal curves (log scale) as expected for typical protein interactions. Binding specificity was evidenced by decreased colorimetric responses in the presence of free IGF-1 (Figure 1), as well as high sodium chloride and high Tween-20 detergent concentrations (data not shown). In the presence of excess glucose or 2-DG (25 – 100 mM), however, the binding of IGFBP-3 to immobilized IGF-1 was unaltered in all cases. As negative controls, microtitre wells lacking immobilized protein or primary/secondary antibodies failed to generate any colorimetric response (data not shown). In the reversed orientation, ELISA assays were also performed in which IGFBP-3 was immobilized (Figure 2). Saturable, dose-dependent binding of IGF-1 was detected and, similar to above, the interaction could be competed with free IGFBP-3 but was unaltered by glucose or 2-DG. ELISA assays were performed in other buffer settings (PBS, Krebs-Ringer) with identical conclusions (data not shown).

Quantitative binding of IGF-1 to IGFBP-3 – To validate the ELISA data, binding between IGF-1 and IGFBP-3 was then examined using label-free, real-time SPR and the identical HBS-EP buffer system. A single, low nanomolar concentration of IGF-1 specifically bound to immobilized IGFBP-3 under high flow rate conditions (Figure 3), whereas an equimolar concentration of BSA failed to interact (i.e. negative binding control). The overall amounts of IGF-1 bound and the individual association and dissociation kinetics were not significantly altered in the presence of excess glucose or 2-DG (25 – 100 mM). Expanding upon the fixed-concentration specificity tests, IGF-1 was then titrated in the absence and presence of excess 2-DG (Figure 4). Visually, the overall dose-dependence and individual kinetics of IGF-1 binding to immobilized IGFBP-3 were not significantly altered in the presence of excess glucose or 2-DG. Likewise, global fitting of each titration series to a 1:1 kinetic model indicated that there was no significant difference in the sub-nanomolar affinity for this interaction over replicate trials (Table I). In the absence or presence of an additional "k_t" parameter, we also confirmed that the curve fitting was not significantly altered by mass transport limitations (i.e. fitted k_t coefficient was ~10^8 RU M^{-1} s^{-1} as expected).

Complex formation between IGF-1 and IGFBP3 – To validate the ELISA and SPR data, we also used Mass Spectrometry (MS) to demonstrate that 2-DG and glucose have no effect on IGF-1/ IGFBP-3 binding. In recent years, Surface Enhanced Laser Desorption/Ionization (SELDI) and Matrix Enhanced Laser Desorption/Ionization (MALDI) Time Of Flight (TOF) MS have become a powerful tool for the investigation of non-covalent protein complexes (17). "Intensity Fading" experiments are a relatively novel technique used to directly visualize protein-protein binding without the use of cross-linkers (18). In these experiments, a fixed concentration of protein A (ideally between 5 and

16 kDa) is incubated with different concentrations of its binding partner B; as the concentration of protein B increases, the intensity of the peak corresponding to protein A slowly diminishes or "fades" (19).

In our MS experiments, we incubated IGF-1 at 13 μM alone, with an equimolar concentration of IGFBP-3 (13 μM), or with excess IGFBP-3 (26 μM) in PBS. Figure 5A shows that the intensity of IGF-1 (7600 Da) fades with increasing concentrations of IGFBP-3 (29000 Da), decreasing from 1000 intensity units to under 50 at the highest IGFBP-3 concentration. Epidermal Growth Factor (EGF; 9 μM) was included as an internal, non-binding control and its intensity (6400 Da) remained unaltered across all IGFBP-3 concentrations. As commonly encounted in "intensity-fading" experiments (18,19), detection of resultant IGF-1/IGFBP-3 complex (36000 Da) was not proportional to theoretical expectations. The same experiments were performed in PBS containing 100mM 2-DG (Figure 5B) or 100 mM glucose (data not shown) and similar spectral outcomes were observed. Since neither glucose nor 2-DG was able to reverse the intensity fading of the IGF-1 peak, this assay indicates that they do not influence IGF-1/IGFBP-3 binding.

Effects of 2-DG on AKT and IGF-1R – Furthermore, we investigated the effect of 2-DG on IGF-1R and AKT activation in two breast cancer cell lines (MCF-7 and T47D) and one cervical cancer cell line (HeLa). We observed that addition of 2-DG at 25 mM, a concentration previously reported to enhance AKT phosphorylation in these cell lines (20), resulted in a consistent decrease in IGF-1R activation. As shown in figure 6, exposure to 2-DG actually reduced IGF-1R beta chain tyrosine 1135/1136 phosphorylation in both basal and IGF-1 (130 nM) stimulated contexts and across all three cell lines. We also observed that AKT activation is not universally induced by 2-DG. Figure 6 shows that phospho-serine 473 AKT is increased in T47D cells and decreased in MCF-7 cells in basal 10% FBS conditions. In IGF-1 (130 nM) stimulated conditions, 2-DG does not appear to have a considerable effect on AKT activation in either MCF-7 or T47D cells. In HeLa cells, AKT phosphorylation is basally high and is not substantially altered in the presence of IGF-1 or 2-DG. These results indicate that 2-DG induced AKT activation is not universal and not IGF-1R dependent, as implied by Zhong et al. Moreover, 2-DG induced activation of 5' adenosine monophosphate activated protein kinase (AMPK) was consistently high across all cell lines (data not shown), which is in agreement with previously published results by Zhong et al. suggesting that 2-DG induced changes in AKT activation are AMPK independent (20).

Discussion

Our main objective was to investigate the effects of 2-DG and glucose on IGF-1/IGFBP-3 binding, as a follow-up to a recent publication by Zhong and colleagues (10). They showed that a concentration of 25 mM 2-DG was sufficient to disrupt more than 60% of IGF-1/IGFBP-3 complexes, a finding which, if confirmed, would have considerable impact both on IGF and cancer research. The reported finding that 2-DG exposure is associated with higher free IGF-1 concentrations challenges its utility as an antineoplastic agent and even its utility as an experimental strategy to selectively inhibit glycolysis without affecting other aspects of cellular physiology. It became important to determine if its relatively well characterized inhibition of glycolysis would predominate over this newly described stimulation in IGF signaling.

We sought to extend the finding of by Zhong and colleagues (10), by indentifying changes in affinity constants and by evaluating the potential effects of glucose, obviously structurally related to 2-DG, on IGF-1/IGFBP-3 complex formation. Using ELISA, we have shown that IGF-1/IGFBP-3 binding is unaltered by either 2-DG or glucose at various concentrations both within and exceeding physiologic range. The assay was performed both in different orientations and in different buffer systems with identical conclusions.

To date, several groups have used SPR to examine the interaction between IGF-1 and its binding proteins (21,22). Similar to the assay design detailed in previous reports, our SPR results are based upon IGF-1 injected over immobilized IGFBP-3 at a high flow rate (75

μL/min) and low signal range (<150 RU) to minimize any potential mass transport effects. Global fitting of the titration series to a 1:1 kinetic model with or without mass transport effects yielded similar outcomes. Our kinetic estimates were biologically-relevant (e.g. k_a ~10^3 – 10^7 $M^{-1}s^{-1}$ and k_d ~10^{-1} – 10^{-6} s-1 for typical protein interactions) and correlated well with values previously reported (21,22) (i.e. overall affinity between IGF-1 and IGFBP-3 is sub-nanomolar). Ultimately, the presence of excess glucose or 2-DG failed to significantly alter the binding interaction between IGF-1 and immobilized IGFBP-3 in our SPR assay.

Using Mass Spectrometry, we demonstrated for the first time that a newer "intensity fading" approach (19) is appropriate for the study of IGF-IGFBP complexes. While the resultant signal for the complexes did not match the anticipated theoretical predictions, this issue has been encountered by others (18,19) and may be the result of higher ionization energies required for complexes compared to the individual protein and its binding partner alone. Nevertheless, our intensity-fading experiments clearly show that the signal corresponding to IGF-1 was decreased in a dose-dependent manner upon IGFBP-3 addition and that 2-DG or glucose had no effect compared to the control MS spectra.

Upon examination of 2-DG induced changes in IGF-1R signaling in MCF-7, T47D and HeLa cell lines, we were unable to confirm the previously published finding that exposure to 2-DG induces IGF-1R activation (10). In fact, we observed that 2-DG treatment reduces phosphorylation of IGF-1R in all three cell lines tested. This finding provides further evidence against the hypothesis that 2-DG disrupts IGF-1/IGFBP-3 complex formation which leads to activation of the IGF-1R. Moreover, the fact that phospho-serine 473 AKT levels changed in a cell specific manner and were uncorrelated with phospho-IGF-1R levels supports the hypothesis that 2-DG induced changes in AKT activation are independent of IGF-1R in these cell lines.

In conclusion, we have utilized three unique experimental strategies to demonstrate that 2-DG does not alter the binding interaction between IGF-1 and IGFBP-3. While our direct measures of IGF-1/IGFBP-3 complex formation contrast with the experimental findings reported by Zhong et al. (10), we suspect that the commercial assay (which was designed to measure free IGF-1 in serum samples) utilized in their study may have been limited by its ability to provide only an indirect measure of IGF-1/IGFBP-3 complex formation. The mechanism responsible for 2-DG induced increase in IGF-1R signaling observed by Zhong and colleagues (10,20) in some cell lines remains unknown. However, our results using several independent methods do not support the hypothesis of a universal mechanism involving IGF-1/IGFBP-3 complex disruption, but rather suggest a mechanism involving cell specific intracellular signaling differences.

Reference List

1. Pollak, M. (2008) *Nat Rev Cancer* **8** (12), 915-928.
2. Laviola, L., Natalicchio, A., and Giorgino, F. (2007) *Curr Pharm Des* **13** (7), 663-669.
3. Collett-Solberg, P.F., Cohen, P. (2000) *Endocrine* **12** (2), 121-136.
4. Vincent, A.M., Feldman, E.L. (2002) *Growth Horm IGF Res* **12** (4), 193-197.
5. LeRoith, D., Roberts, C.T., Jr. (2003) *Cancer Lett* **195**, 127-137.
6. Ghosh, P., Dahms, N.M., and Kornfeld, S. (2003) *Nat Rev Mol Cell Biol* **4** (3), 202-212.
7. Firth, S.M., Baxter, R.C. (2002) *Endocr Rev* **23**, 824-854.
8. Hwa, V., Oh, Y., and Rosenfeld, R.G. (1999) *Endocr Rev* **20** , 761-787.
9. Jones, J.I., Clemmons, D.R. (1995) *Endocr Rev* **16** (1), 3-34.
10. Zhong, D., Xiong, L., Liu, T., Liu, X., Liu, X., Chen, J., Sun, S.Y., Khuri, F.R., Zong, Y., Zhou, Q., and Zhou, W. (2009) *J Biol Chem* **284** (35), 23225-23233.
11. Wick, A.N., Drury, D.R., and Morita, T.N. (1955) *Proc Soc Exp Biol Med* **89** (4), 579-582.
12. Wick, A.N., Drury, D.R., Nakada, H.I., and Wolfe, J.B. (1957) *J Biol Chem* **224** (2), 963-969.

13. Chen, W., Gueron, M. (1992) *Biochimie* **74** (9-10), 867-873.
14. Singh, D., Banerji, A.K., Dwarakanath, B.S., Tripathi, R.P., Gupta, J.P., Mathew, T.L., Ravindranath, T., and Jain, V. (2005) *Strahlenther Onkol* **181** (8), 507-514.
15. Myszka, D.G. (1999) *J Mol Recognit* **12** (5), 279-284.
16. Levitt, R.J., Georgescu, M.M., and Pollak, M. (2005) *Biochem Biophys Res Commun* **336** (4), 1056-1061.
17. Bolbach, G. (2005) *Curr Pharm Des* **11** (20), 2535-2557.
18. Yanes, O., Nazabal, A., Wenzel, R., Zenobi, R., and Aviles, F.X. (2006) *J Proteome Res* **5** (10), 2711-2719.
19. Yanes, O., Villanueva, J., Querol, E., and Aviles, F.X. (2007) *Nat Protoc* **2** (1), 119-130.
20. Zhong, D., Liu, X., Schafer-Hales, K., Marcus, A.I., Khuri, F.R., Sun, S.Y., and Zhou, W. (2008) *Mol Cancer Ther* **7** (4), 809-817.
21. Beattie, J., Phillips, K., Shand, J.H., Szymanowska, M., Flint, D.J., and Allan, G.J. (2008) *Mol Cell Biochem* **307** (1-2), 221-236.
22. Vorwerk, P., Hohmann, B., Oh, Y., Rosenfeld, R.G., and Shymko, R.M. (2002) *Endocrinol* **143** (5), 1677-1685.

FOOTNOTES

*We would like to thank the Genome Quebec & Lady Davis Institute Clinical Proteomics facility for the help with mass spectrometry experiments. Sheldon Biotechnology Centre is supported by a Research Resource Grant (RRG) from the CIHR.

The abbreviations used are: 2-DG, 2-deoxy-D-glucose; ELISA, enzyme-linked immunosorbant assay; IGF-1, insulin-like growth factor 1; IGFBP-3, IGF binding protein 3; k_a, association rate constant; k_d, dissociation rate constant; k_t, mass transport coefficient, K_D, equilibrium dissociation constant; MS, mass spectrometry; RU, resonance unit; SPR, surface plasmon resonance.

FIGURE LEGENDS

FIGURE 1 – **ELISA assay to monitor binding of IGFBP3 (0 – 1000 nM in HBS-EP) to immobilized IGF-1 in the absence (open squares) or presence of 100 mM 2-DG (open triangles), 100 mM glucose (open circles), and 500 nM IGF-1 (closed squares).** Error bars (standard deviation of triplicate measurements) are only depicted for the "Control" and "500 nM IGF-1" series for simplicity.

FIGURE 2 – **Reverse ELISA assay to monitor binding of IGF-1 (0 – 5000 nM in HBS-EP) to immobilized IGFBP-3 in the absence (open squares) or presence of 100 mM 2-DG (open triangles), 100 mM glucose (open circles), and 500 nM IGFBP-3 (closed squares).** Error bars (standard deviation of triplicate measurements) are only depicted for the "Control" and "500 nM IGFBP-3" series for simplicity.

FIGURE 3 – **SPR analysis to monitor specificity of IGF-1 (25 nM in HBS-EP) binding to IGFBP-3 (1000 RU amine-coupled) in the absence (upper solid line) or presence of 100 mM 2-DG (dashed line) and 100 mM glucose (dotted line) at 75 µL/min.** As a negative binding control, no significant response was observed with 25 nM BSA (bottom solid line). Double-referenced data is representative of duplicate injections acquired from two independent trials.

FIGURE 4 – **SPR analysis to monitor real-time kinetics of IGF-1 (0 – 25 nM in HBS-EP; 2-fold dilution series) binding to IGFBP-3 (1000 RU amine-coupled) in the absence (solid lines) or presence of 100 mM 2-DG (dashed lines) at 75 µL/min (3.5 min association + 10 min dissociation).** Double-referenced data is representative of duplicate injections acquired from two independent trials.

FIGURE 5 – **MS analysis to monitor binding between IGF-1 (~7,600 Da) and IGFBP-3 (~29,000 Da) in the absence or presence of 100 mM 2-DG (and internal EGF non-binding control, ~6,400 Da).** *A.* Upper boxes represent 13 nM IGF-1 alone, middle boxes represent 13 nM IGF-1 with 13 nM IGFBP-3, and lower boxes represent 13 nM IGF-1 with 26 nM IGFBP-3. *B.* Identical intensity-fading experiments performed in the presence of 100 mM 2-DG. The data presented is representative of three independent experiments. Y-axes are representative of signal response (uA) and X-axes are representative of molecular mass (Da).

FIGURE 6 – **Western Blot assay of IGF-1R signaling.** MCF-7, T47D and Hela cell lines were plated at 10^6 cells/well in 6-well plates in DMEM media containing 10% FBS. The following day, cells were treated with 10% FBS DMEM media containing 2-DG (25 mM), IGF-1 (130 nM) or both. Four hours later, cells were harvested and levels of signaling proteins were assayed by Western Blot.

TABLE I

Apparent kinetics of IGF-1 binding to immobilized IGFBP-3 in the absence and presence of 2-DG, as assessed by SPR[a]

100 mM 2-DG	k_a x 10^6 M^{-1} s^{-1}	k_d x 10^{-4} s^{-1}	K_D (pM)
-	1.40 +/- 0.01	8.40 +/- 0.04	604 +/- 5
+	1.33 +/- 0.01	7.93 +/- 0.05	599 +/- 5

[a]Estimates (+/- standard error of the mean; n=4) represent global analysis of titration series to a "1:1 kinetic" model where goodness-of-fit (Chi^2) values were <1.5; association rate (k_a), dissociation rate (k_d), and equilibrium dissociation ($K_D = k_d / k_a$) constants were not significantly altered in the presence of an additional mass transport (k_t ~10^8 RU M^{-1} s^{-1}) fitting parameter.

FIGURE 1

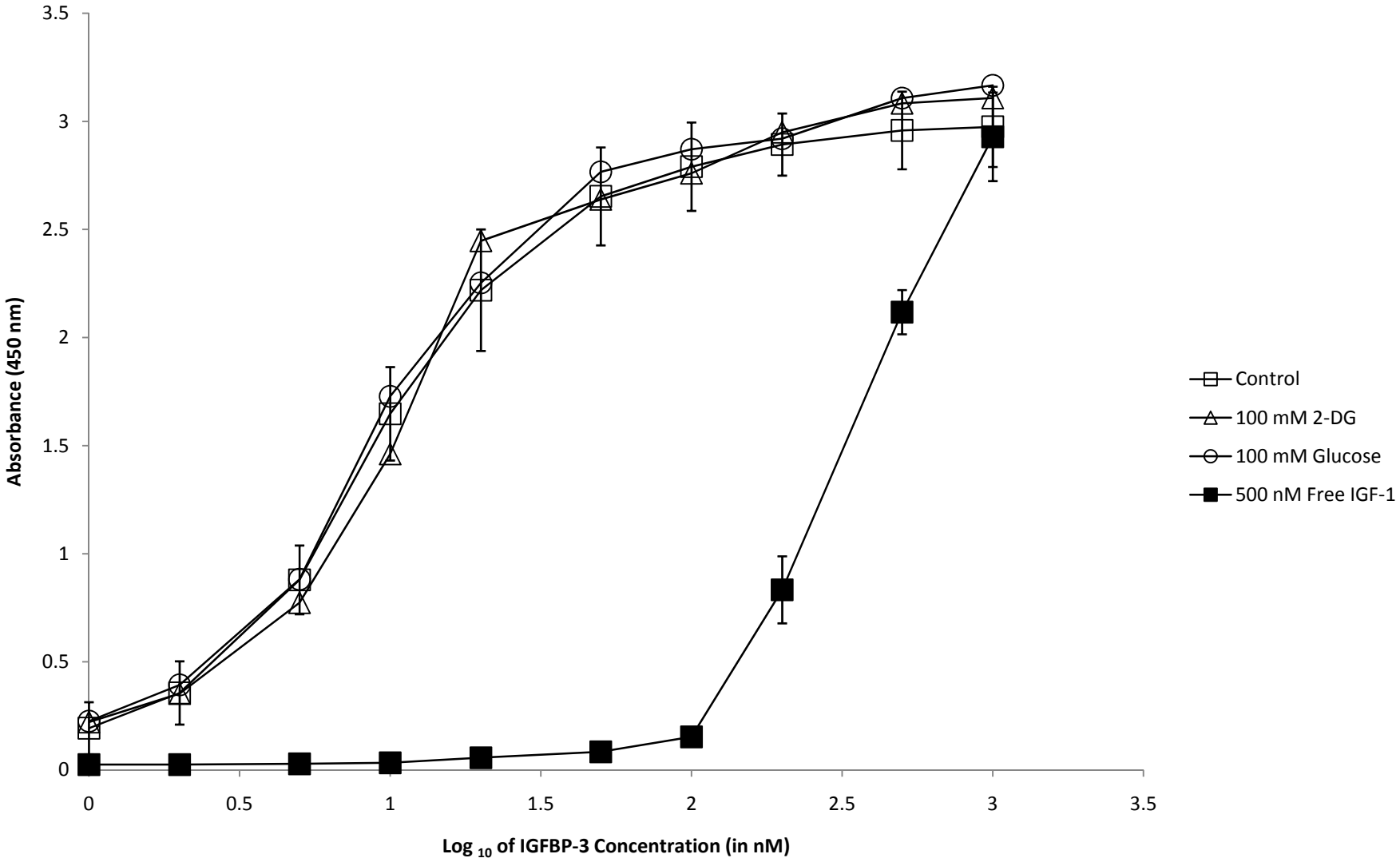
3.5
3
2.5
2
1.5
1
0.5
0
Absorbance (450 nm)
0
0.5
1
1.5
2
2.5
3
3.5
Log 10 of IGFBP-3 Concentration (in nM)
Control
100 mM 2-DG
100 mM Glucose
500 nM Free IGF-1

FIGURE 2

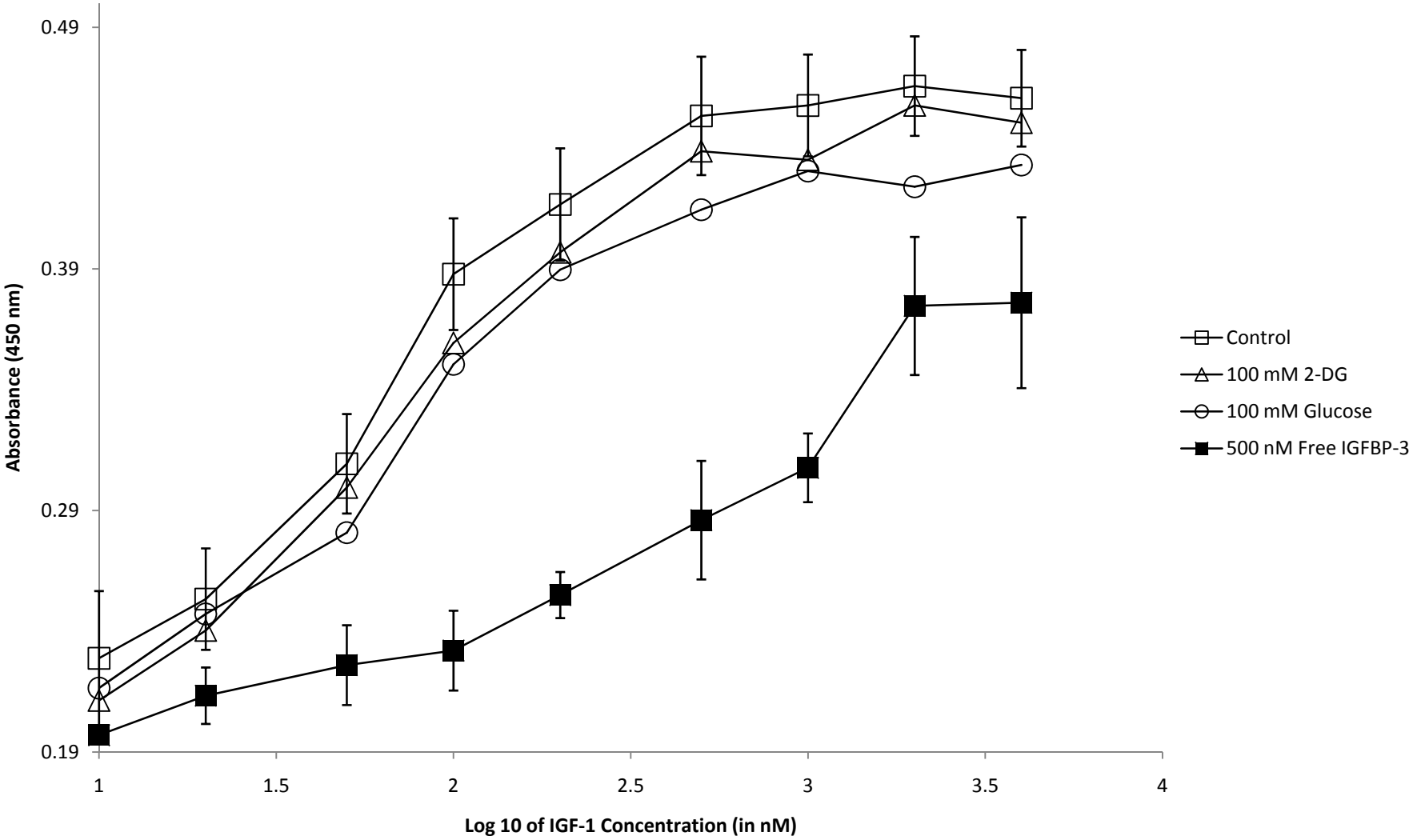
0.49
0.39
0.29
0.19
Absorbance (450 nm)
1
1.5
2
2.5
3
3.5
4
Log 10 of IGF-1 Concentration (in nM)
Control
100 mM 2-DG
100 mM Glucose
500 nM Free IGFBP-3

FIGURE 3:

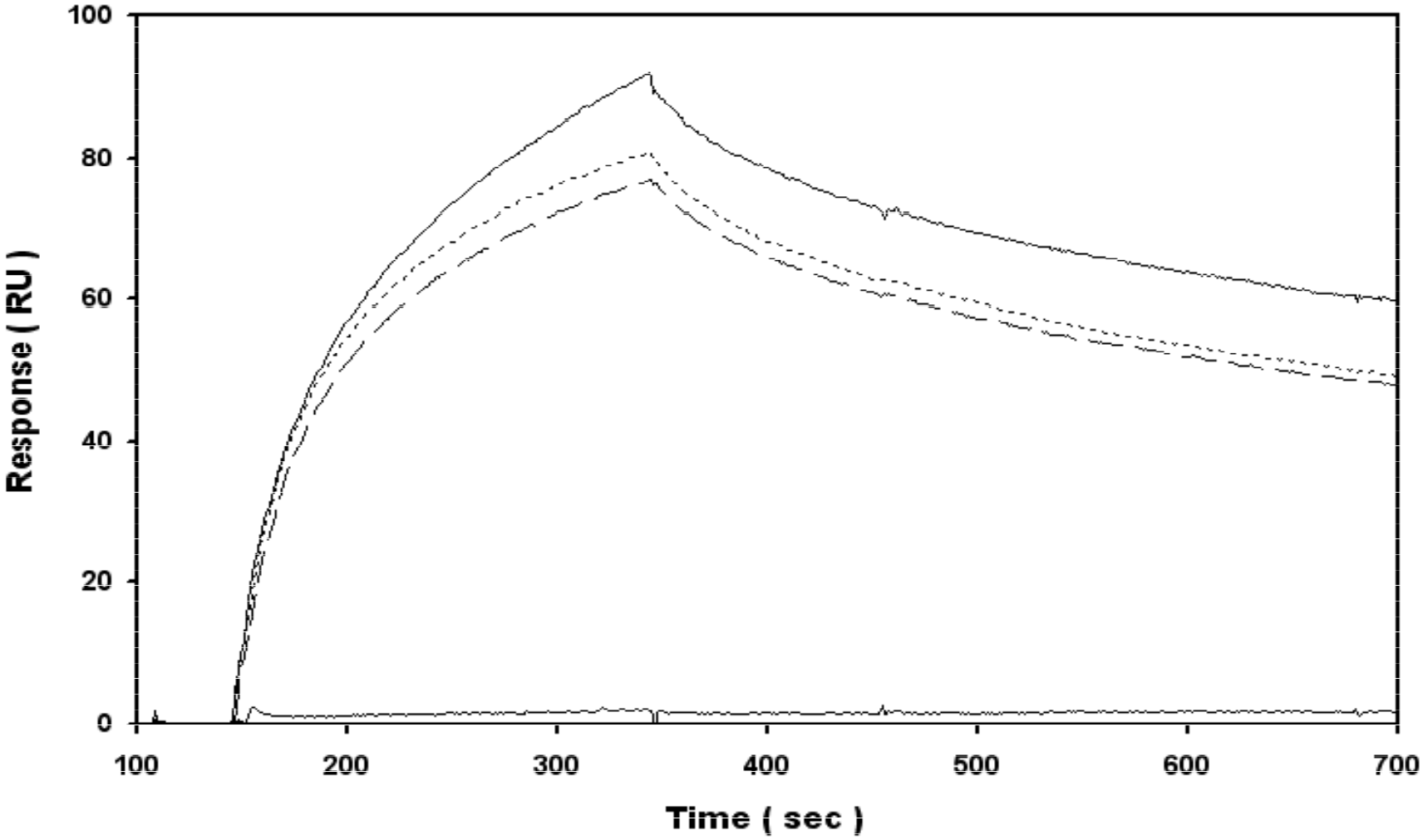
100
80
60
40
20
0
Response (RU)
100
200
300
400
500
600
700
Time (sec)

FIGURE 4:

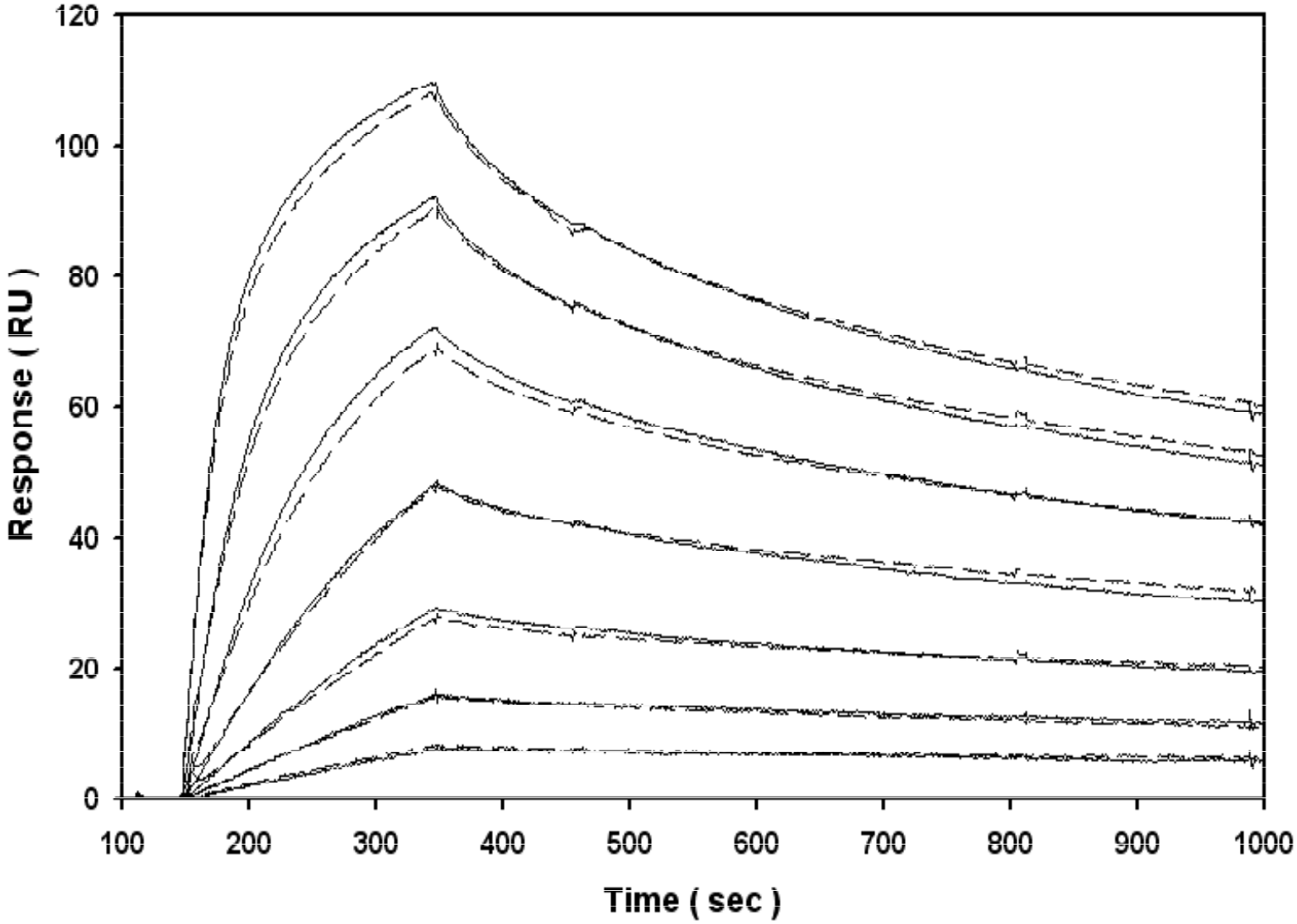
120
100
80
60
40
20
0
Response (RU)
100
200
300
400
500
600
700
800
900
1000
Time (sec)

FIGURE 5

A)

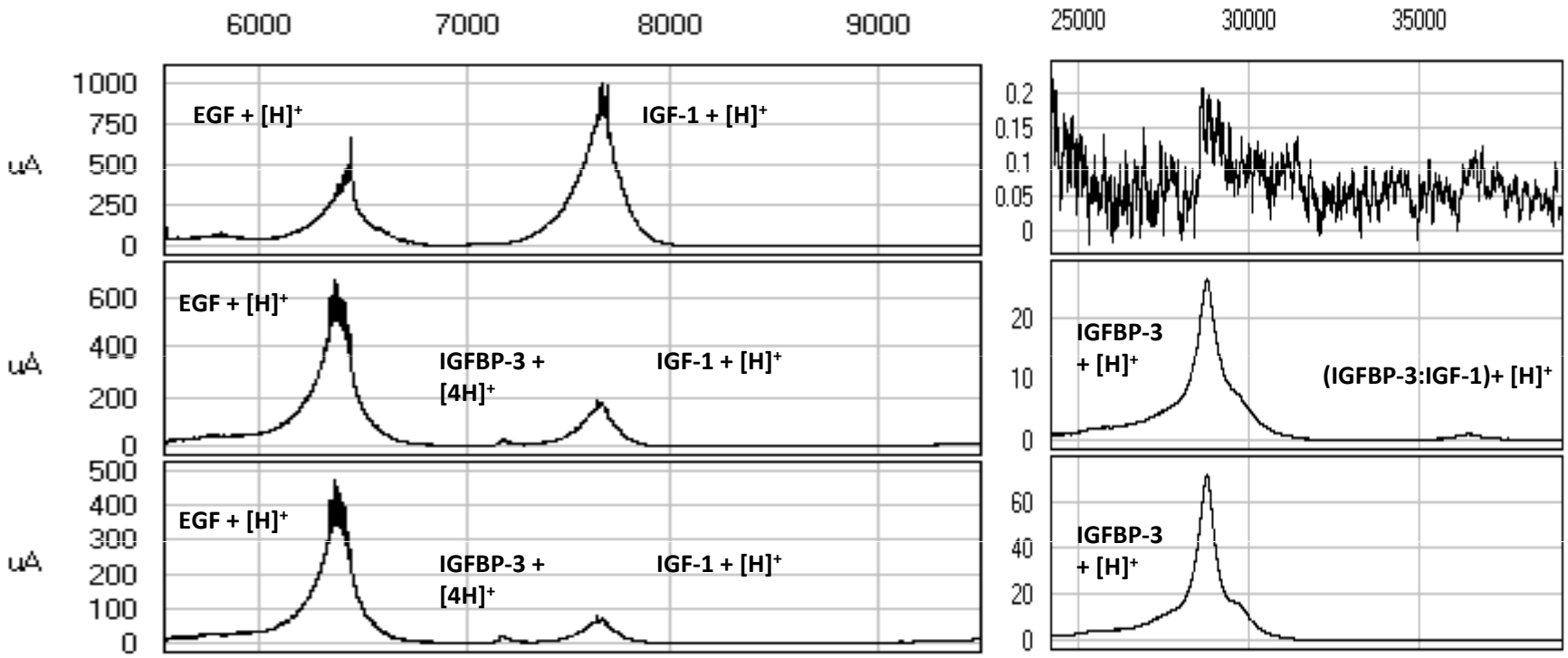
6000
7000
8000
9000
25000
30000
35000
uA
1000
750
500
250
0
EGF + [H]+
IGF-1 + [H]+
0.2
0.15
0.1
0.05
0
600
400
200
0
EGF + [H]+
IGFBP-3 +
[4H]+
IGF-1 + [H]+
20
10
0
IGFBP-3
+ [H]+
(IGFBP-3:IGF-1)+ [H]+
500
400
300
200
100
0
EGF + [H]+
IGFBP-3 +
[4H]+
IGF-1 + [H]+
60
40
20
0
IGFBP-3
+ [H]+

B)

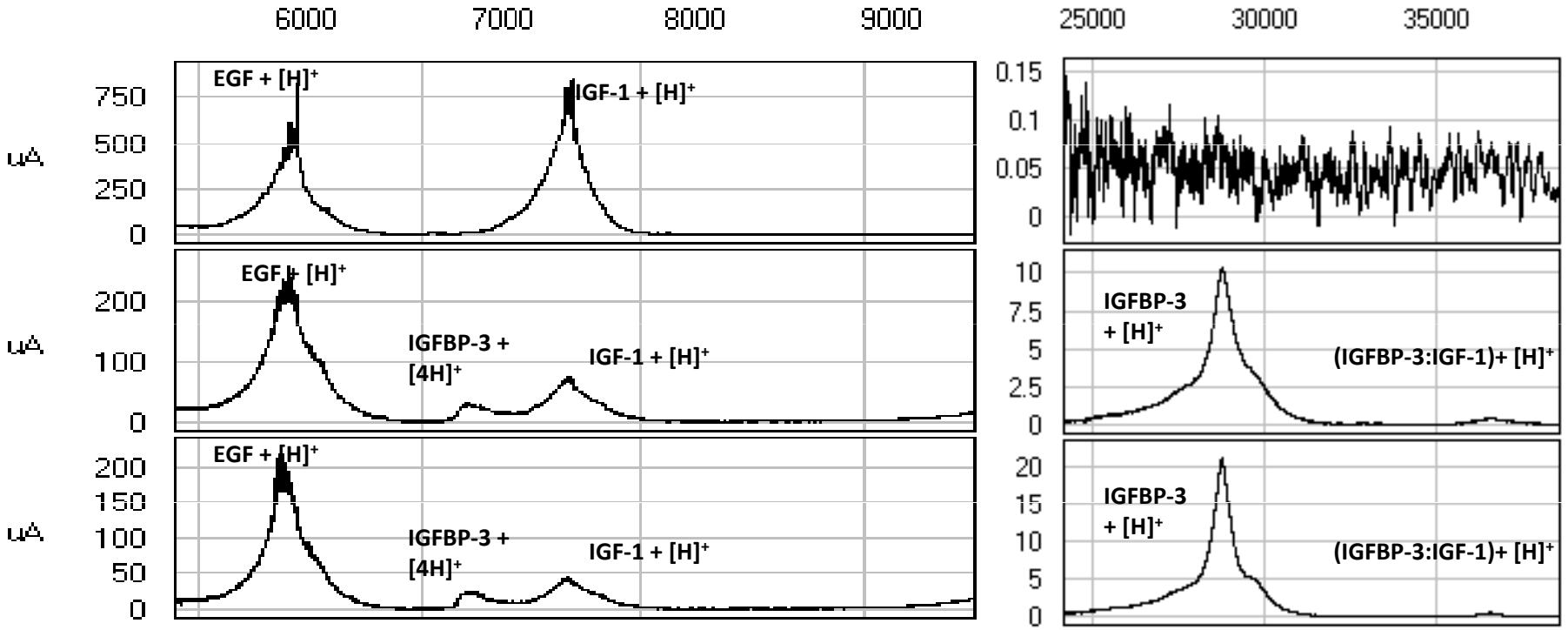
6000
7000
8000
9000
25000
30000
35000
uA
750
500
250
0
EGF + [H]+
IGF-1 + [H]+
0.15
0.1
0.05
0
200
100
0
EGF + [H]+
IGFBP-3 +
[4H]+
IGF-1 + [H]+
10
7.5
5
2.5
0
IGFBP-3
+ [H]+
(IGFBP-3:IGF-1)+ [H]+
200
150
100
50
0
EGF + [H]+
IGFBP-3 +
[4H]+
IGF-1 + [H]+
20
15
10
5
0
IGFBP-3
+ [H]+
(IGFBP-3:IGF-1)+ [H]+

FIGURE 6:

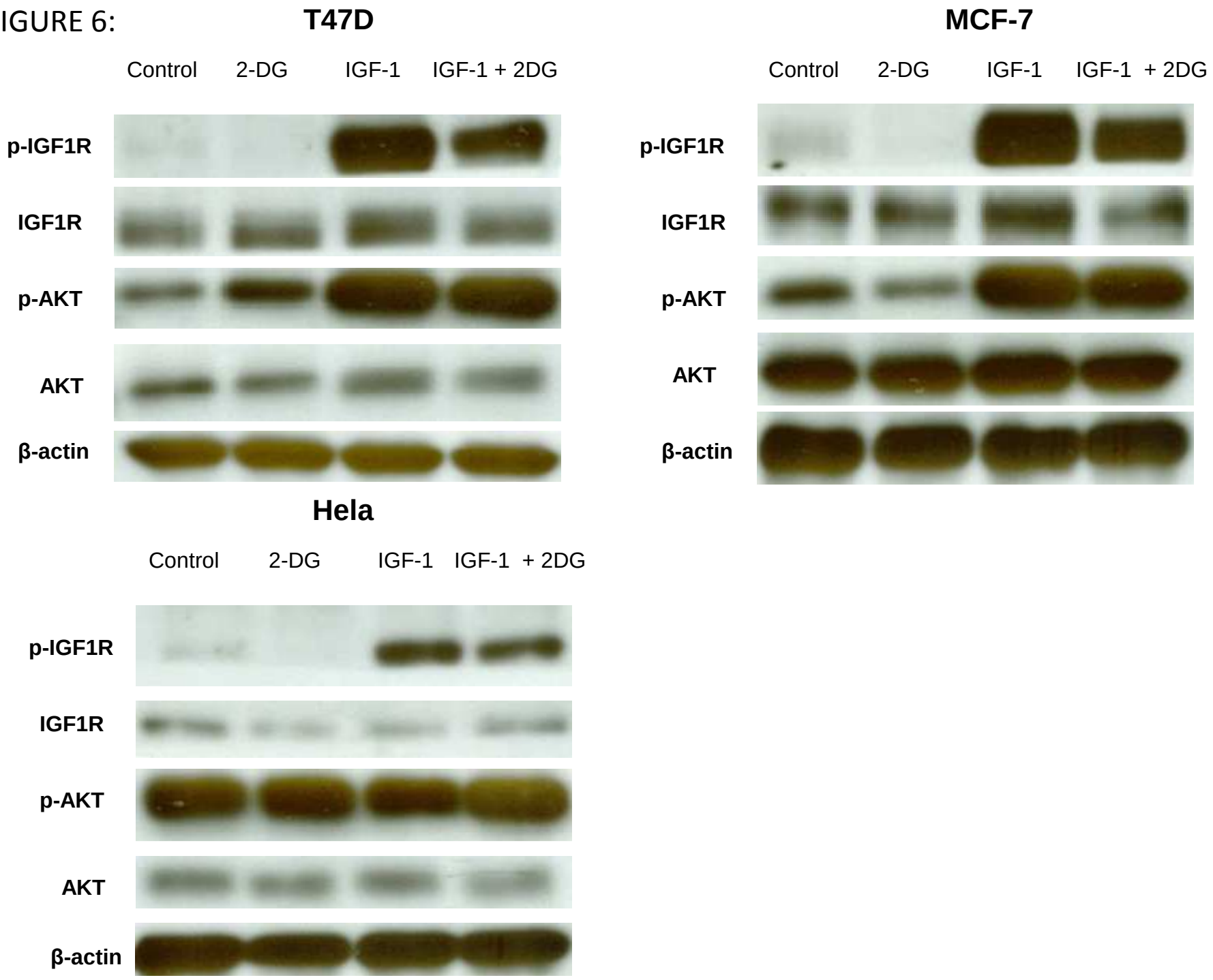
T47D
Control
2-DG
IGF-1
IGF-1 + 2DG
p-IGF1R
IGF1R
p-AKT
AKT
β-actin
MCF-7
Control
2-DG
IGF-1
IGF-1 + 2DG
p-IGF1R
IGF1R
p-AKT
AKT
β-actin
Hela
Control
2-DG
IGF-1
IGF-1 + 2DG
p-IGF1R
IGF1R
p-AKT
AKT
β-actin